International Journal of Quantum Technologies ISSN: 3069-9090

PRIME OPEN ACCESS

Volume 2, Issue 2

Research Article

Date of Submission: 01 May, 2026
Date of Acceptance: 25 May, 2026
Date of Publication: 05 Jun, 2026

Positronium (Ps) Lifetime of 1.7-13 Days on Earth Agrees with 4.3 Days Measured on Global Alfven Waves Radiating to Distant Radio Telescopes

Gerald A. Smith*, D. Drake, D. Mc Devitt, K. Meyer, G. Spalek, D. Barnes and N. Moon

Positronics Research LLC, Unit 109, 7175 E. Camelback Rd., Scottsdale, AZ 85251.

***Corresponding Author:** Gerald A. Smith, Positronics Research LLC, Unit 109, 7175 E. Camelback Rd., Scottsdale, AZ 85251.

Citation: Smith, G. A., Drake, D., Mc Devitt,, D., Meyer, K., Spalek, G., et al., (2026). Positronium (Ps) lifetime of 1.7-13 days on Earth agrees with 4.3 days measured on global Alfven waves radiating to distant radio telescopes. *Int J Quantum Technol, 2*(2), 01-08.

Abstract

In 2026 G. Smith published magnetometer data showing Ps circulating on Earth's 0.4G magnetic field between Scottsdale AZ and Easter Is. Chile with a 4.3+-2.5 days individual Ps lifetime [1]. In an earlier experiment in 2008 in Santa Fe, NM our team found a 2 days Ps lifetime. Since we have modified this result to 1.7-13 days, discussed in detail in the text below. A few of the sections have been "yellowed" to help the reader follow the arguments to their intended end.

Introduction

In Santa Fe, NM our goal was to make stable Positronium on Earth. Para-positronium (pPs) decays quickly with a 125 ps vacuum lifetime. After 50+ns ortho-positronium (oPs) with a 142ns lifetime reaches thermal equilibrium, during which time it decays naturally or quenches with electrons [2]. Existence of oPs lifetimes at room temperature (RT) is known [3]. However, at low temperature (LT) it is relatively scarce. Only limited data are available at 4 and 14K [4,5]. Anti-hydrogen experiments provide some information but without lifetimes and above 4K [6].

We carried out a comprehensive study of oPs lifetimes in Silica Aerogel (SA) at 4K in our Santa Fe laboratory. From independent experiments it is shown that oPs are very cold. This paper reports on a subset of lifetimes measured in a weak remnant paramagnetic field. The field, the strength of which is enhanced at LT, is due to unprecedented levels of β^+ radiation absorbed in a strong magnetic field forming a material called "quasi-ferromagnetism".

The following questions are addressed in this paper: What is the paramagnetic free electron density resulting from the radiation? What is the remnant magnetic field formed in the strong applied Fe magnetic field? What are the oPs equilibrium energies and yields? Can the remnant field influence oPs lifetimes? How do measured lifetimes and yields compare with theory?

Experimental Details

Apparatus

The apparatus consisted of a super-conducting solenoid magnet, β^+ sources, SA and a positron annihilation lifetime spectrometer (PALS) [2]. The 1st magnet cool-down used 2 mm diameter, side-by side 45μCi ^{22}Na sources, sandwiched between 25.4 μm Kapton films in 10^{-4} torr vacuum. A slot in the vertical cold bore (Figure 1a) held the source disk (Figure 1b), with two 0.1 g/cc SA cells, above and below each source between thin aluminum plates. The 2nd cool-down used a single 10 mm diameter, 18 uCi source with two 0.05 g/cc SA cells, one above and one below. Pore diameters of the 0.1 and 0.05 g/cc SA were, on average, 20 and 40 nm, respectively.

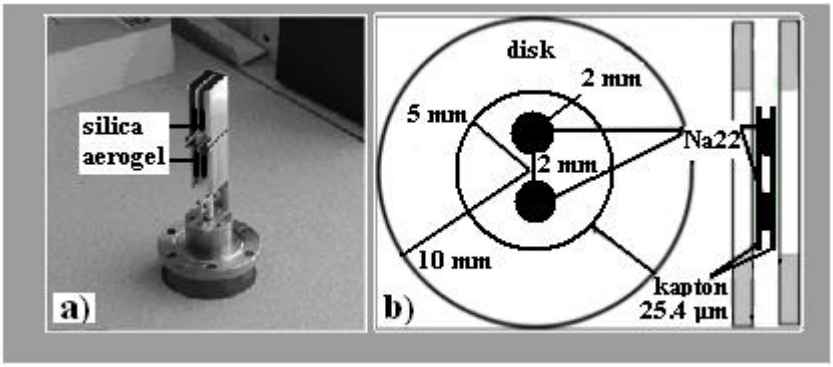

Figure 1: a) Magnet Cold-Bore Showing Slot for Source Disk and Four Silica Aerogel Cells and b) ^{22}Na Source Disk Dimensions

The PALS system included two BaF_2 cylindrical scintillators, 5.1 cm in diameter and 4.3 long, on XP2020Q PM tubes placed up to 50 cm from the sources depending on desired rates. MCA data from an Ortec 566 TAC, using discriminated 'start' and 'stop' signals from 1274 and 511 keV γ rays, respectively, were recorded. Co^{60} γ-rays gave a FWHM time resolution of 422 ps. While larger by sometimes a factor of two compared to other systems, it is perfectly adequate for measuring lifetimes upwards of a factor of one hundred times larger. Time spectra were fitted with Positronfitto a set of four decays: pPs, 'free' annihilation, oPs pickoff and oPs, the potential source of stable Positronium [7]. Time resolution was sent to Positronfit and subtraction of accidentals background was made by fitting 200 ns of TAC output before the start pulse.

Behavior of β^+ in the Silica Aerogel

GEANT4 was used to predict positron motion and radiation dose in the SA. Figure 2 shows ten randomly selected ^{22}Na β^+ in the 0.1 g/cc setup at 3T field. Eight are tightly pinned to field lines in the vacuum due to interaction of their transverse momentum with the field. Multiple coulomb scattering is evident after they enter the SA cells. Straight lines are back-to-back annihilation γ-rays. Two annihilate in the source or Kapton windows, giving 80% β^+ stopping in SA.

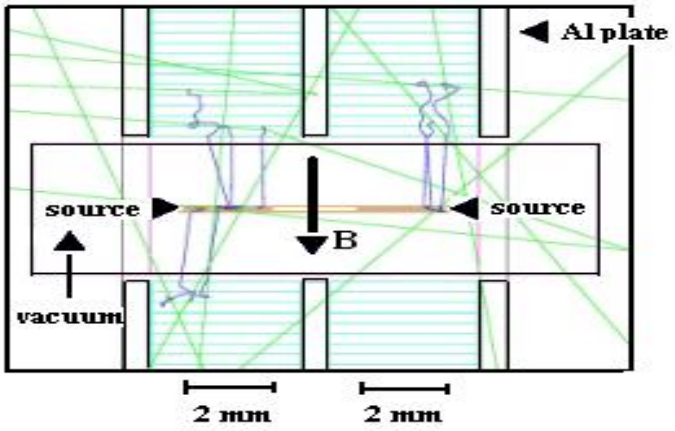

Figure 2: GEANT-4 simulation of ten β^+ from Two 2mm, 45μCi ^{22}Na Sources in 0.1g/cc Silica Aerogel (shaded areas) at 3T; Straight Lines Are Back-to-Back Annihilation γ-rays; Aluminum Plates that hold the SA are shown; the Area between the Sources and SA is in Vacuum as Indicated.

Figure 3 shows the computed dose rate for the 0.1 and 0.05 g/cc setups versus penetration depth. Each SA cell was divided into a lattice with unit dimensions of 0.02 (x) x 0.05 (y) x 0.005 (z) cm^3, where z is parallel to B. Without the field the exponential absorption coefficients are computed to be 4.90 and 2.45 cm^{-1}, respectively [8]. Fits to Figure 3 give 11 ± 2 and 7 ± 1 cm^{-1}, respectively, showing shortening of penetration depth by factors of two-three due to the 3T field.

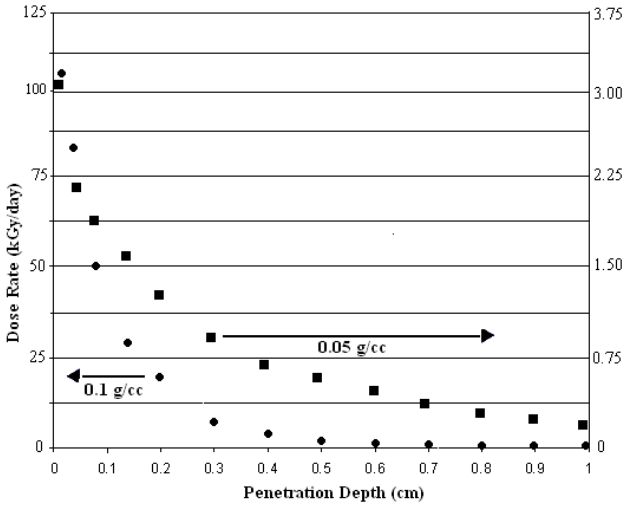

Figure 3: GEANT-4 Simulated Dose Rates Versus Penetration Depth for 0.1 g/cc SA (Solid Circles/Left Scale) and 0.05 g/cc SA (Solid Squares/Right Scale)

Including 90% β^+ branching ratio and 8 keV energy loss in the source and window, the daily peak dose for the 0.1 g/cc setup in the first layer of the lattice is 90 μCi x 3.7 x 10^4 Bq/μCi x 0.9 x 0.8 x 24 h/d x 3600 s/h x 192 keV x 1.6 x 10^{-16} J/keV x 10^3 Gy-g/J x 1/[4 cells x π(0.10 cm)^2 x (0.005 cm) x 0.1 g/cm^3 = 101±25 kGy/day. The peak rate for the 0.05 g/cc setup is obtained by scaling from 0.1 g/cc: 18/90 x 4 cells/2 cells x (0.1/0.5)2 x 0.1/0.05 x 101±25 = 3.2±0.8 kGy/day.

Quasi-Ferromagnetic Fields

In a strong applied magnetic field, the radiation dose is expected to produce a paramagnetic magnetization M, given by $M = n_e \mu_B L$, where n_e is electron density, μ_B is the electron magnetic moment and L(a) is the Langevin function with $a = n_e \mu_B B/NkT$ [9]. With $\mu_B = 9.27 \times 10^{-24}$ A-m^2, B = 3 T, N = 3 x 10^{27} atoms-m^{-3} in 0.1 g/cc SA, k = 1.38x10^{-23}J/K and T = 4 K, $a = 1.68 \times 10^{-28} n_e$.

EPR data from electron irradiation of silica (2.2 g/cc) at RT are used to determine n_e. After 1900 kGy dose (see Run 15, Table 1), scaling to 0.1 g/cc density gives n_e (RT) = (4.0±0.7) x 10^{23} x 0.1/2.2 = 1.8±0.3 x 10^{22} m^{-3} [9]. Stability is several weeks, and is expected to be longer at LT [10]. Since low energy electron/positron energy loss is virtually identical, this applies to β^+ also.

We may correct n_e to LT using known oPs-pPs conversion rates at 14K [4]. During application of 6 kGy dose from ^{22}Na to SA, the rate increased by a factor of 10^3 due to increase of electron density. Scaling to 1900 kGy gives n_e (LT) = (1.8±0.3) x 10^{22} x 10^3 x 1900/6 = 5.7±2 x 10^{27}m^{-3}.

Finally, the remnant field is determined by substituting n_e (LT) from above into the expression for a, giving a = 0.6±0.2, or L = 0.2. Therefore, M = (5.7±2) x 10^{27} x 4.27 x 10^{-24} x 0.2 = (4.9±1.5) x 10^3 T-A2/N, or $B_{rem} = 4\pi \times 10^{-7} M$ = 61±12G.

Independently, exposure of silicon/silica at 10 K to 4x10^{16} thermal neutrons/cm^2, estimated at 6±1 kGy dose, produces hysteresis with B_{rem} = 4.4 G [11,12]. Scaling to 0.1 g/cc density and 1900 kGy gives Brem = 4.4 G x 0.1/2.2 x 1900/6 = 63±15 G. Agreement of the two estimates leads us to adopt B_{rem} = 60 G for Run 15. Conversion is given by B_{rem}(G) = 0.031 x Dose (kGy).

Quality of Lifetime Fits

Because of the importance of measured lifetimes to this study, we carefully review two lifetime fits. First, Figure 4 shows the Run 6 (see Table 1) lifetime distribution with a complete set of fitted lifetime values shown in the inset. Errors compare favorably with an independent Monte Carlo analysis [13]. With 5% signal and constant background, scaling for event number gives a Monte Carlo oPs lifetime error of ±28 ns, in good agreement with a fitted value of ±27 ns.

Second, the TAC measures time from a start pulse to the next stop pulse. If either input receives random pulses in addition to valid pulses, it analyzes the first pulse and suppresses later pulses. This distorts the measured lifetime distribution for correlated valid starts and stops. An expression for the observed distribution, in terms of total start ns and stop ne rates, and valid start nV and stop ne' rates, has been derived [14,15].

Equation (3) of ref. requires rates from separate gated energy measurements [16]. The start energy spectrum (Figure 5a) is well accounted for by Monte Carlo simulation. However, the stop energy spectrum (Figure 5b) below 400 keV significantly exceeds the simulation due to accidental counts. The following rates were determined from Figure 5: n_s = 3,700 s^{-1}, n_e = 5,300 s^{-1}, n_V = 3,500 s^{-1}, n_e' = 3,500 s^{-1} and $\varepsilon_s = n_e'/n_s$ = 0.95.

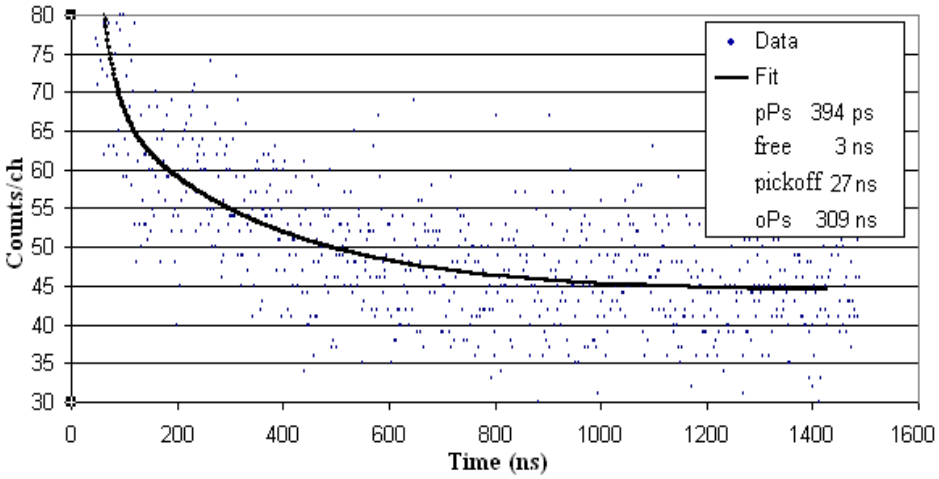

Figure 4: Run 6 Field-Off Lifetime Distribution: 87.6% Fit Probability; TAC < 2000 ns; Fitted Lifetimes are shown in the Inset

Equation (3) is valid provided $n_e'\tau < \Delta\tau/\tau$, where $\Delta\tau/\tau$ is the measured fractional lifetime error. At 309 ns, $n_e'\tau = 0.0011$, which is less than 27 ns/309 ns by a factor of eight. Therefore, the observed spectrum per unit time is: $n(t) = \exp(-n_e t)$ [A $\exp(-t/\tau)$+B], where $A = n_V \varepsilon_s(n_s+1/\tau)$ and $B = n_V n_e(1-\varepsilon_s)$. Since $\varepsilon s \approx 1$, $n_e\tau << 1$, and $1/\tau >> n_s$, n(t) simplifies to A $\exp(-t/\tau)$, with $A = n_V/\tau = 11.3\pm3.2$ ns^{-1}. Substituting, n(309 ns) = 11.3±3.2 ns^{-1} x e^{-1} x 1.95 ns/ch = 9.4±2.7 counts/ch. From Figure 4 the signal above background is 9 counts/ch x 1.06 = 9.5 cts/ch, where a separately determined dead time correction factor is included. The probability these two rates agree is 97%.

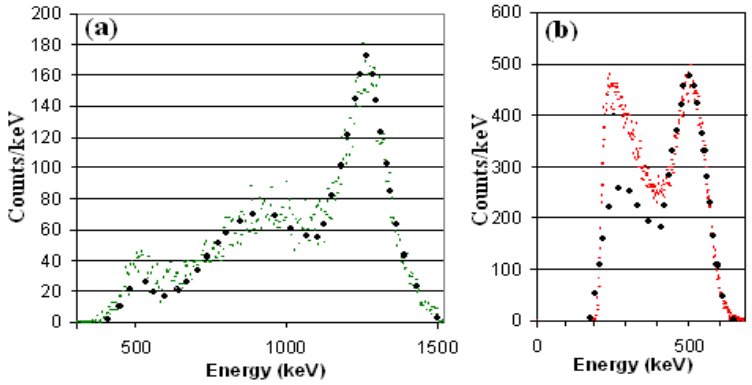

Figure 5: Run 6 Gated (a) Start and (b) Stop Energy Distributions with Monte Carlo simulations (Solid Circles) Normalized to (a) Prompt 1274 keV and (b) 511 keV Ps Decay Peaks.

Figure 6 shows the Run 14 lifetime distribution and fit. Gated energy distributions give n_s = 8,700 s^{-1}, ne = 18,000 s^{-1}, n_V = 8,200 s^{-1}, n_e' = 8,000 s^{-1} and ε_s = 0.9. At 687 ns, $n_e'\tau = 0.0055$ is a factor of twenty-two less than $\Delta\tau/\tau$ = 81 ns/687 ns. Therefore, the same approximations apply as in Run 6, with A = 11.9±3.3 ns, and n(687) = 11.9±3.3 ns^{-1} x e^{-1} x 1.95 ns/ch = 8.5±2.4 counts/ch. From Figure 6, including a dead time correction, the signal above background is 9.5 counts/ch x 1.08 = 10.3 counts/ch. The statistical probability that these two rates agree is 45%. In summary, the oPs lifetime fits to Runs 6 and 14 reflect the true nature of the spectra.

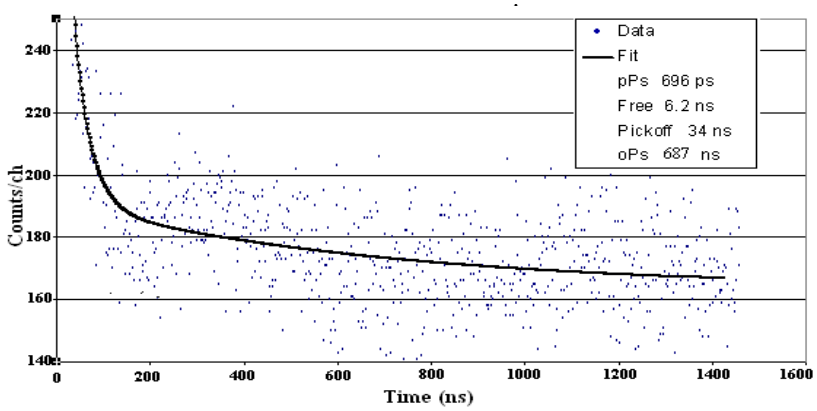

Figure 6: Run 14 Field-off Lifetime Distribution: 21.8% Fit Probability; TAC <2000 ns; Fitted Lifetimes are shown in the Inset

Results

We now present oPs lifetime results. Data were taken intermittently with field-on runs in 23 and 66 consecutive day intervals of the 1st and 2nd magnet cool downs, respectively. Fifteen field-off runs with high quality fits (>10% probability) are listed in Table 1 in chronological order for each cool down. Runs 13-15, 1-12, were recorded in the 1st, 2nd cool downs. Doses are determined by multiplying maximum dose rates (101 and 3.2 kGy/d respectively) by the number of exposure days. Remnant fields are given by B_{rem}(G) = 0.031 x Dose (kGy), as discussed in the next section.

A striking feature of Table 1 is two tightly bunched and well-separated lifetime groups, one of six runs (3,7,9-11,12) with lifetimes less than 142 ns (75±3 ns average) and a second of nine runs (1,2,4-6,8,13-15) with lifetimes greater than 142 ns (356±20 ns average). Discussion in the next section shows that the groups arise from a selection wherein oPs velocities may or may not be above a magnetic field dependent critical threshold for formation of long-lived states.

Run	Dose*(kGy)	Lifetime(ns)	Yield (%)
1	32	267±36	2.4±0.1
2	32	287±41	2.4±0.2
3	35	69±4	5.6±0.6
4	38	400±37	2.7±0.1
5	99	190±16	2.4±0.1
6	118	309±27	5.5±1.7
7	118	66±4	3.4±0.1
8	118	234±31	2.3±0.1
9	192	51±5	1.2±0.1
10	192	122±44	0.9±0.3
11	208	82±6	2.0±0.1
12	208	62±3	2.1±0.1
13	1515	441±121	4.1±0.7
14	1717	687±81	4.1±0.2
15	1919	389±41	3.1±0.2

Table 1: Field-off runs: 500 ns <TAC < 2,000 ns; Fit Probability>10%; *Maximum Dose with Maximum Remnant Field Given by B_{rem}(G) = 0.031 x Dose(kGy) (see text for details)

Discussion

Previous Results

To place the problem in context, we review equilibrium temperatures from other experiments. Extrapolation of kT* from 19 keV β^+ energy to 100 keV (^{22}Na) in silica powder (0.18 g/cc) at 4.2 K gives kT* = 0.6±0.4 meV [17,18]. Further, in silica powder with ^{22}Na at 4.5 K, differences in RT and 4.75 K decay rates give kT* = 13±7 meV [3,19]. The average, corrected for density, is kT* = 7±5 x $(0.18/0.1)^{2/3}$ = 10±7 meV, with a mean velocity v_m = 4.2±3.5 x 10^4 m/s [18].

In addition, 7 keV β^+ in oxidized silicon (1.9 g/cc) at 150 K give kT* = 145±10 meV , and 10 keV β^+ in silica film (1.5 g/cc) at 50 K give kT* = 48±5 meV [19,20]. Both results fall on a universal curve, kT*(meV) = 1.1T(K), confirming the previous result of 10±7 meV at 4K.

Finally, yields are characterized by $[T/T^*]^{2-2m}/\Gamma(3-2m)$ [21]. At 4.2K, above 0.9 meV the energy spectrum is described by m = -1. Substituting T = 4K and T* = 15.6K, the yield is 2.3%. Recent results at 13K and 10 keV in silica film give 2.5% [22]. Both agree with values in Table 1.

Summarizing, at 4 K cold oPs made by ^{22}Na β^+ in 0.1 g/cc SA has an equilibrium energy of kT* = 10±7 meV and a yield of a few percent.

Field-Theoretic Trapping Model

A non-relativistic field theory, with crossed electric (E) and magnetic (B) fields, has been found to explain our recent results, thereby setting conditions for Ps confinement in general [2,22]. With E = 0, B along +z and electron-positron separation along -x, the invariant pseudo-momentum (au) is

$$K_y = 2v_y + \frac{B}{2}x. \quad (1)$$

The effective potential may be written [23]

$$V(x,0,0) = \frac{B^2}{4}x^2 + \frac{BK}{2}x + \frac{K^2}{4} - \frac{1}{\kappa x}, \tag{2}$$

where κ-1 = 0.34 for SA at 0.35 g/cc density and 4 K [22], or scaling to 0.1 g/cc density, $\kappa \approx 1$.

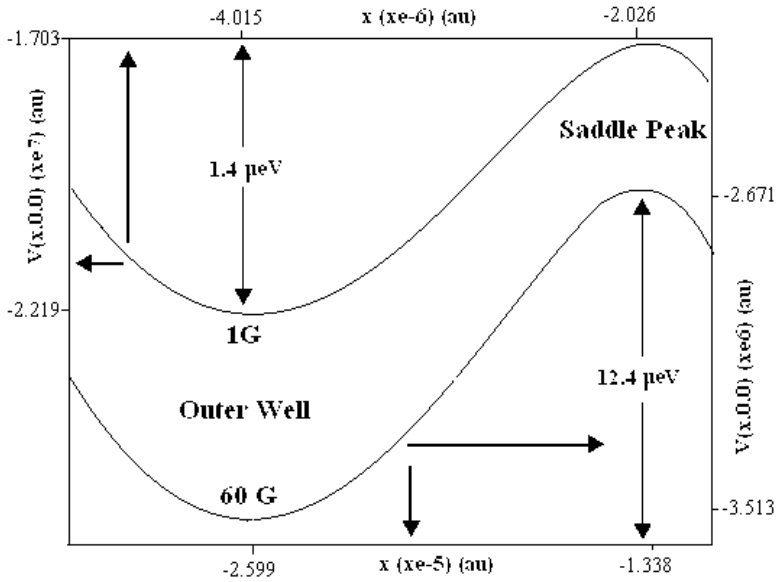

Figure 7: Effective Potential for Brem = 1 G (K = 0.0020 au) and 60 G (K = 0.0078 au), E = 0

Figure 7 illustrates V(x,0,0) for B_{rem} = 1 and 60 G. At the high extreme (60 G, Run15), the critical value K_c, above which an outer well (OW) exists, is $(27B/2)^{1/3}$ = 0.0070 au [23]. With K = 0.0078 au the OW is centered at x_o = -260,000 au (-13.8μm) and V_o = -3.5 x 10-6 au (-95 μeV), with the saddle peak at x_s = -134,000 au (-7.1μm) and V_s = -2.7 x 10^{-6} au (-73 μeV). At the low extreme (1 G Runs 1-4), with K_c = 0.00179 au and K = 0.0020 au, the curve is similar in shape to 60 G. However, x_o and x_s are larger, and V_o and V_s smaller, by factors of fifteen and nine, respectively. Well depths of 12.4 μeV (60G) and 1.4 μeV (1G) bear directly on collision stability.

The ionization energy of the states in Figure 7 are I = B, or +2.6 x 10^{-8} au (+0.69 μeV) and +4.3 x 10^{-10} au (+0.12 μ eV) for 60 G and 1 G, respectively [23]. With Vs < I, both are low energy saddle states (LESS), with shared probability among the magnetically distorted coulomb well (MDCW), barrier and OW regions [24]. As K increases, xo moves toward the origin, and V_s increases until it equals I, at which point transformation to an OW is complete.

Solving eq. (1) for x_o = -260,000 au and B = 60 G, v_y = 0.0056 au (1.22 x 10^4 m/s). With v_m = 4.2±3.5 x 10^4 m/s, the fraction of oPs in a Maxwell-Boltzmann (MB) distribution with velocity greater than v_y is 99^{+1}_{-79} %. This also applies to 1 G, where v_y = 0.0014 au (3.12 x 10^3 m/s). Therefore, both agree with 60±18% (9/15 runs) for lifetimes greater than 142 ns in Table 1.

No other oPs lifetime measurements exist with a magnetic field in SA at LT, and only one exists at RT. At 2.9 kG the lifetime is reported as 51 ns (no error), with estimated average oPs energy≈50 meV [3]. This is consistent with an earlier measurement of 50±10 meV in SA at RT, but with no magnetic field [24]. At K = 0.03 au, just above threshold, the LESS velocity is 9.3 x 10^4 m/s. With v_m = (9.5±1.9) x 10^4 m/s for the MB distribution, the probability that an oPs will not form a LESS is 42^{+12}_{-11} %. The likelihood of one measurement occurring at 51 ns is large.

Summarizing, oPs transitions to LESS at 1-60 G result from the fact that the mean oPs velocity at 4K is well above the weak field dependent critical velocity. No other existing experiments in laboratory magnetic fields contradict or confirm this result. Because of the probabilistic spread of velocities, an ensemble of measurements is required for this purpose.

Lifetimes

The square of the ratio of Ps to LESS ground state wave functions at the origin, $|\psi_{Ps}(0)/\psi_{LESS}(0)|^2$, is $(x_{n=1}/x_o)^{-3}$, or $(2/4{,}015{,}000)^{-3} = 8.1 \times 10^{18}$ (1 G) and $(2/260{,}000)^{-3}$ = 2.2 x 10^{15} (60 G). Lifetimes can be estimated by multiplying by the 5 ns spin-averaged Ps lifetime, giving vacuum lifetimes of 131yrs and 13dys, respectively. These are foreshortened by classical electron and positron synchrotron radiation to [τ = 17 dy/γB(G)] 17 yrs and 1.7 dys (γ = 1), respectively.

Actual lifetimes depend on quenching mechanisms. The first is collision breakup in the silica. The maximum energy transfer in an elastic collision is $\Delta E = 8m_eE/M$ [5]. For E = 10±7 meV and M ≈ 23 amu [3], ΔE = 1.9±1.3 μeV, well

below the 12.4 μeV well depth (60 G), but comparable to 1.4 μeV (1 G). Therefore, a LESS is stable at 60 G (Runs 13-15), but at 1-6 G (Runs 1-12) for a uniformly populated well, the probability of survival is ≈ [1 - (1.9±1.3 -1.4)/1.4] = 64^{+36}_{-64}%.

The second quenching mechanism is pickoff. In analogy to oPs, scaling from RT to 4 K and from 70 to 20 nm pores, the pickoff rate in SA is λ_{po} = 0.4 μs^{-1} x $(4/300)^{1/2}$ x 70/20 = 0.16 μs^{-1} [4]. For comparison, silica (2.2 g./cc) at 20 K, with density and temperature scaling, gives λ_{po} = 11.2 μs^{-1} x 0.1/2.2 x $(4/20)^{1/2}$ = 0.23 μs^{-1}. For further considerations we assume λ_{po}= 0.20 μs^{-1} [25].

The final and important mechanism is wall collisions. For the 1st cool down setup, the maximum distance traveled by a LESS from the SA surface to a plate is 25 mm. The corresponding lifetime, corrected for pickoff, is 2.5 cm/ [(4.2±3.5) x 10^6 cm/s] x exp (-0.2μs^{-1} x 0.500 μs) = 536±446 ns. The minimum lifetime from the SA back to the source in vacuum is 0.6 cm/ [(4.2±3.5) x 10^6 cm/s] = 143±119 ns. The average lifetime of 506±40 ns for Runs 13-15 is within these bounds.

An analysis for the 2nd cool-setup gives a maximum predicted lifetime of 389±324 ns, after correcting by 0.64 for collision losses in silica. The minimum is the same as for the 1st cool down. The average lifetime of 281±50 ns for Runs 1,2,4-6, and 8 is within minimum and maximum bounds. Thus, long lifetimes are due to wall collisions, corrected for pickoff and silica collisions.

Conclusions

Loosely bound electrons from β^+ radiation in an applied magnetic field produce, depending on irradiation time, 1-60 G peak remnant quasi-ferromagnetic fields in silica aerogel at 4K. Two lifetime groups are observed with field-off, one oPs-like and the other with longer lifetimes. Sixty percent of oPs have velocities above critical values for these fields, leading to long-lived saddle states with 1.7-13 days lifetime predicted by theory. Observed lifetimes result from wall annihilations, with contributions from collisions and quenching. Yields are a few percent.

By comparison, working in Earth's magnetic field and atmospheric plasma protects stable Ps from particle and radiative collisions and hence break-up inherent to the laboratory experiment apparatus described herein is not applicable. An experiment done recently by a member of our group gives 4.3+-2.0 days stable Ps lifetime [1]. This compares favorably with our 1.7-13 days lifetime described herein. Both experiments agree with Shertzer et al and da Silva et al theories [22,23].

Acknowledgements

This work was supported by US Air Force Research Laboratory contracts F08630-01-C-0028 and F08630-02-C-0018. The authors are grateful to K. Edwards (AFRL) and M. Stickley (DARPA) for their steadfast support. Advice from D. Schrader on theory is appreciated. Helpful suggestions on an early version of the paper by M. Charlton were useful in preparing the final manuscript.

References

1. Smith, G. A. (2026). Long Lived Positronum on Earth's Magnetic Field Confirms Equal Antimatter, Matter Gravity and Intraplanetary Double Helix Radio Waves. Int J Quantum Technol, 2(1), 01-06.
2. Charlton, M., & Humberston, J. W. (2001). Positron physics (Vol. 11). Cambridge University Press.
3. Nagashima, Y., Kakimoto, M., Hyodo, T., Fujiwara, K., Ichimura, A., Chang, T., ... & Stewart, A. T. (1995). Thermalization of free positronium atoms by collisions with silica-powder grains, aerogel grains, and gas molecules. Physical Review A, 52(1), 258.
4. Saito, H., & Hyodo, T. (2001). Cooling and quenching of positronium in porous material. In New Directions in Antimatter Chemistry and Physics (pp. 101-114). Dordrecht: Springer Netherlands.
5. Saito, H., Nagashima, Y., Hyodo, T., & Chang, T. (1995). Detection of paramagnetic centers on amorphous-SiO 2 grain surfaces using positronium. Physical Review B, 52(2), R689.
6. Brusa, R., Mariazzi, S., Consolati, G., Dupasquier, A., Quasso, F., & Giammarchi, M. (2008). Production of cold positronium atoms. Acta Physica Polonica A, 113(5), 1301-1306.
7. Kirkegaard, P., & Eldrup, M. (1972). POSITRONFIT: A versatile program for analysing positron lifetime spectra. Computer Physics Communications, 3(3), 240-255.
8. Horodek, P., & Dryzek, J. (2010). GEANT4 simulation of implantation profiles for positrons injected in solids from radioactive sources 22Na and 68Ge/68Ga. Nukleonika, 55(1), 17-19.
9. Elliott R S 1966 *Electromagnetics,* McGraw-Hill, p. 427-33
10. Agnello S, Gelardi F M, Boscaino R, Cannas M, Boizot B and Petite G 2002 *Nucl. Inst. Meth. B* **191** 387
11. Pfeffer R L 1965 *J. Appl. Phys.* **57** 3176
12. Klett, A., & Burgkhardt, B. (1996, November). The new remcounter LB6411: measurement of neutron ambient dose equivalent H*(10) according to ICRP60 with high sensitivity. In 1996 IEEE Nuclear Science Symposium. Conference Record (Vol. 1, pp. 132-134). IEEE.
13. Dubroca, T., Hack, J., Hummel, R. E., & Angerhofer, A. (2006). Quasiferromagnetism in semiconductors. Applied physics letters, 88(18).
14. Thraenert S, Hassan E M and Krause-Rehberg R. 2006 *Nucl. Inst. Meth. B* **248** 336

15. Paul, D. A. L. (1977). On the analysis of decay time coincidence spectra. Journal of Physics E: Scientific Instruments, 10(4), 412-415.
16. Coleman, P. G. (1979). The distortion of TAC-MCA spectra by the measuring process. Journal of Physics E: Scientific Instruments, 12(7), 590-592.
17. MILLS, A., & Shaw, E. D. (1989). RS CI':'SCHESTER, DM ZUCKERMAN. Phys. Rev., B, 40, 2045.
18. Kiefl, R. F., & Harshman, D. R. (1983). Positronium in SiO2 powder at low temperature. Physics Letters A, 98(8-9), 447-450.
19. Mariazzi, S., & Brusa, R. S. (2011, January). o-Ps cooling for antihydrogen production. In Journal of Physics: Conference Series (Vol. 262, No. 1, p. 012037).
20. Crivelli, P., Gendotti, U., Rubbia, A., Liszkay, L., Perez, P., & Corbel, C. (2010). Measurement of the orthopositronium confinement energy in mesoporous thin films. Physical Review A—Atomic, Molecular, and Optical Physics, 81(5), 052703
21. Mariazzi, S., Toniutti, L., Patel, N., & Brusa, R. S. (2008). Formation and escaping of positronium in porous SiO2 films at low temperature. Applied surface science, 255(1), 191-193.
22. Shertzer, J., Ackermann, J., & Schmelcher, P. (1998). Positronium in crossed electric and magnetic fields: The existence of a long-lived ground state. Physical Review A, 58(2), 1129.
23. da Silva A, dos Santos D and Aegerter M 1987 *Non-Cryst. Sol.* **95-96** 1159
24. Chang, T., Xu, M., & Zeng, X. (1987). Effect of the energy loss process on the annihilation of orthopositronium in silica aerogel. Physics Letters A, 126(3), 189-194.
25. Dutta, D., Ganguly, B., Chatterjee, S., & Mukherjee, T. (2005). Effect of temperature on positronium annihilation in silica gel. The Journal of Physical Chemistry B, 109(20), 10092-10095.